

NMR Evidence of Antiferromagnetism in $\text{Nd}_{0.85}\text{Sr}_{0.15}\text{NiO}_2$

Yi Cui,^{1,*} C. Li,^{1,*} Q. Li,^{2,*} Xiyu Zhu,² Z. Hu,¹ Yi-feng Yang,³
J. S. Zhang,⁴ Rong Yu,^{1,†} Hai-Hu Wen,^{2,‡} and Weiqiang Yu^{1,§}

¹*Department of Physics and Beijing Key Laboratory of Opto-electronic Functional Materials & Micro-nano Devices, Renmin University of China, Beijing, 100872, China*

²*National Laboratory of Solid State Microstructures and Department of Physics, Center for Superconducting Physics and Materials,*

Collaborative Innovation Center for Advanced Microstructures, Nanjing University, Nanjing 210093, China

³*Beijing National Laboratory for Condensed Matter Physics and Institute of Physics, Chinese Academy of Sciences, Beijing 100190, China*

⁴*Mathematics and Physics Department, North China Electric Power University, Beijing 102206, China*

Despite the recent discovery of superconductivity in $\text{Nd}_{1-x}\text{Sr}_x\text{NiO}_2$ thin films, the absence of superconductivity and antiferromagnetism in their bulk materials remain a puzzle. Here we report the ^1H NMR measurements on powdered $\text{Nd}_{0.85}\text{Sr}_{0.15}\text{NiO}_2$ samples by taking advantage of the enriched proton concentration after hydrogen annealing. We find a large full width at half maximum of the spectrum, which keeps increasing with decreasing the temperature and exhibits an upturn behavior at low temperatures. The spin-lattice relaxation rate $1/T_1$ is strongly enhanced when lowering the temperature, developing a broad peak at about 40 K, then decreases following a spin-wave-like behavior $1/T_1 \sim T^2$ at lower temperatures. These results evidence a quasi-static antiferromagnetic ordering of magnetic moments below 40 K and dominant antiferromagnetic fluctuations extending to much higher temperatures. Our findings reveal the strong electron correlations in bulk $\text{Nd}_{0.85}\text{Sr}_{0.15}\text{NiO}_2$, and shed light on the mechanism of superconductivity observed in films of the nickelate.

The recent discovery of superconductivity in films of the infinite layer nickelate $\text{Nd}_{1-x}\text{Sr}_x\text{NiO}_2$ [1, 2] with a maximal transition temperature T_c of 14.9 K has attracted a lot of research attention. $\text{Nd}_{1-x}\text{Sr}_x\text{NiO}_2$ has the same lattice structure as the infinite-layer cuprate superconductor $(\text{Sr}_{1-x}\text{Ca}_x)_{1-y}\text{CuO}_2$ [3]. In the undoped NdNiO_2 , the Ni^{1+} ion has an electron configuration of $3d^9$ with a single hole in the $d_{x^2-y^2}$ orbital, as Cu^{2+} in cuprate superconductors. It was proposed that upon Sr^{2+} substitution for Nd^{3+} the nickelate behaves as a doped Mott insulator, in analogy to the hole-doped cuprates [4]. However, a number of major differences between these two systems have been noted. The charge transfer gap between the Ni $3d$ to O $2p$ orbitals was estimated to be much larger than that in cuprates [5, 6]. So it is under debate whether the hole introduced by Sr doping would reside on the O site as in cuprates [7], or on the Ni site forming a $3d^8$ configuration. The latter could cause an $S = 1$ high-spin $3d^8$ configuration of Ni that involves multiorbital physics [5, 8–13]. Moreover, the larger charge transfer gap leads to a smaller exchange energy [14, 15], which may substantially suppress the antiferromagnetism in the nickelate. In addition, the $5d$ [16, 17] and $4f$ [18] electrons in Nd^{3+} , and/or interstitial s electrons [19] may also participate to the low-energy electronic structure.

The above concerns put it an open question the doped Mott insulator scenario of the nickelate and stimulates alternative theoretical proposals involving Kondo effect [11, 12], anti-Kondo effect [18], multi-orbital effect [20, 21], Hund's coupling [22], and disorder effect. Surprisingly, more recent measurements on the bulk ma-

terials show absence of superconductivity [23] and no long-range order antiferromagnetism [24–26]. These results not only challenge the similarity between nickelates and cuprates, but also raise an intriguing question: what could be the critical ingredients manipulating the superconductivity in film and bulk nickelates.

Both the $\text{Nd}_{1-x}\text{Sr}_x\text{NiO}_2$ films and the powdered bulk crystals are made from $\text{Nd}_{1-x}\text{Sr}_x\text{NiO}_3$ by post annealing in hydrogen atmosphere to remove the apical oxygen in the lattice [2, 23–25]. However, the resistivity of the powdered bulk crystals show an insulating behavior from room temperature down to 1.5 K. One may wonder the role of hydrogen annealing: besides removing the apical oxygens, could it be a key factor of tuning the superconductivity by introducing effective charge doping or inhomogeneity?

Experimental studies on the electronic structure and magnetism are very demanded to address the above questions and to get a convergent understanding of the superconductivity in the nickelates. NMR is an ideal probe of low-energy physics in condensed matter systems, and the hydrogen annealing motivates us to search for ^1H NMR in bulk $\text{Nd}_{0.85}\text{Sr}_{0.15}\text{NiO}_2$ samples, whose film counterpart is near optimal doping [2].

In this manuscript, we show that the ^1H NMR intensity of $\text{Nd}_{0.85}\text{Sr}_{0.15}\text{NiO}_2$ is much larger than that of $\text{Nd}_{0.85}\text{Sr}_{0.15}\text{NiO}_3$, which implies a higher concentration of hydrogen after annealing. More strikingly, although the hyperfine shift 1K_s in the annealed sample is very small, a large increase of full width at half maximum (FWHM) of the spectrum is observed in $\text{Nd}_{0.85}\text{Sr}_{0.15}\text{NiO}_2$. The spin-lattice relaxation rate is very

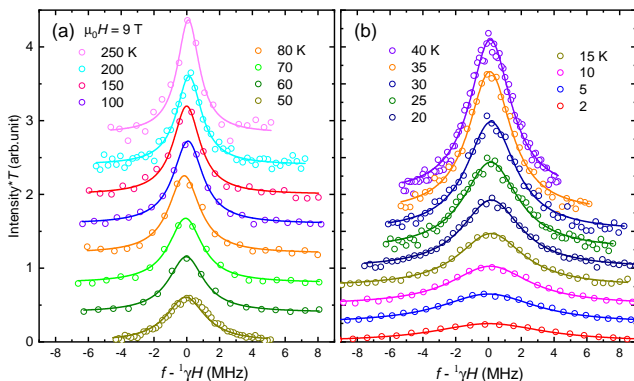


FIG. 1: The ^1H NMR spectra (open circles) of $\text{Nd}_{0.85}\text{Sr}_{0.15}\text{NiO}_2$ at a fixed field of $\mu_0 H = 9$ T, obtained by frequency sweep at selected temperatures. The NMR intensity is obtained from the integration of the spin-echo spectrum multiplying by the temperature. For clarity, vertical shifts are applied to data at different temperatures, and vertical scales in panels (a) and (b) are chosen differently. The solid lines are function fits to the spectra with the single-Lorentzian form.

high, and is largely enhanced with decreasing the temperature, developing a broad peak at about 40 K. These results, together with the extracted Korringa ratio far below 1, signals dominant antiferromagnetic (AFM) fluctuations in the system. Below 40 K, the FWHM of the spectrum increases dramatically with an upturn behavior, and the $1/T_1 \sim T^2$ showing a spin-wave-like behavior. These suggest a quasi-static AFM order developing below 40 K. The observed enhanced AFM fluctuations and the quasi-static AFM ordering are inherent in the strong electron correlations in bulk materials, and are crucial for the understanding of the magnetism and superconductivity in nickelates.

The powdered samples of $\text{Nd}_{0.85}\text{Sr}_{0.15}\text{NiO}_2$ in this study are made by the topotactic hydrogen annealing method as reported in earlier papers [23, 27]. In principle it is hard to perform NMR measurements on $\text{Nd}_{0.85}\text{Sr}_{0.15}\text{NiO}_2$ without isotope enrichment. But after annealing, hydrogen can be injected to the system given its small size. Taking this advantage, ^1H (spin-1/2, $\gamma = 42.5759$ MHz/T) NMR signal is found by using a standard spin-echo pulse sequence $\pi/2 - \tau - \pi$, where $\pi/2$ and π pulse lengths are $1.5 \mu\text{s}$ and $3.0 \mu\text{s}$, respectively, and $\tau \sim 1 \mu\text{s}$ is the blank time between two pulses. Such short pulses and τ are selected to minimize the 1T_2 effect which is found to be about $20 \mu\text{s}$ at low temperatures. The full NMR spectrum is obtained by frequency sweep at a fixed field. The spin-lattice relaxation rate 1T_1 is measured by the inversion-recovery method, and the spin-recovery is fitted by stretched exponential functions, with a large stretching factor $\beta \sim 0.3$, indicating either magnetic anisotropy or sample inhomogeneity. In addition to this short 1T_1 NMR signal, a long 1T_1 component with a narrow bandwidth (about 100 kHz) is also

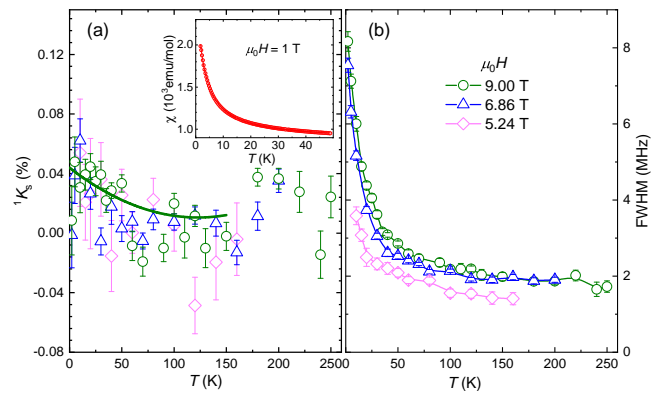


FIG. 2: (a) The NMR hyperfine shift of $\text{Nd}_{0.85}\text{Sr}_{0.15}\text{NiO}_2$ as functions of temperatures at different fields. The solid line is a polynomial fit to the 9 T data below 150 K. Inset: the susceptibility as a function of temperature with a fixed field $\mu_0 H = 1$ T. (b) The FWHM of the spectra of $\text{Nd}_{0.85}\text{Sr}_{0.15}\text{NiO}_2$ as functions of temperatures.

found, which we believe comes from the environment. For each NMR measurement, the spectrum is taken after a sequential $\pi/2$ pulse and a short recovery time to remove the background environment ^1H signal. The magnetization data are measured by a VSM in a Quantum Design PPMS (physical property measurement system).

The ^1H NMR spectra measured by frequency sweep under a constant field 9 T and various temperatures are shown in Fig. 1, where zero frequency corresponds to zero Knight shift. Upon cooling, the NMR spectra follow the Lorentzian form and barely shift with temperature. The hyperfine shift K_s (defined as $K_s = f_p/\gamma H - 1$, where f_p is the peak frequency of the spectrum) and the FWHM are then calculated from the spectra. Their temperature evolutions at several fields are shown in Fig. 2(a) and Fig. 2(b), respectively. K_s is very small, with a typical value less than 0.1%. Yet a weak upturn upon cooling is still resolved, which is consistent with the increase of the measured bulk susceptibility data (inset of Fig. 2). The small K_s values and the upturn behavior barely depend on the field. On the other hand, as shown in Fig. 2(b) the FWHM is much larger than the hyperfine shift (relative to the zero frequency), as shown in Fig. 1, and increases with decreasing temperature from 250 K to 40 K, indicating a large magnetic broadening of the spectra.

Below 40 K, the FWHM increases rapidly with decreasing the temperature and follows an upturn behavior. Such a large broadening is a typical character of inhomogeneous NMR linewidth, as is much bigger than the measured $1/T_2$ ($T_2 \approx 20 \mu\text{s}$ at low temperatures). This large linewidth and the upturn behavior are observed over a broad field range. Though the powdered sample is chemically and structurally inhomogeneous, the strong temperature dependence of the FWHM below 40 K at large fields can only be attributed to a precursor to static AFM ordering, because in an antiferromagnet, the pro-

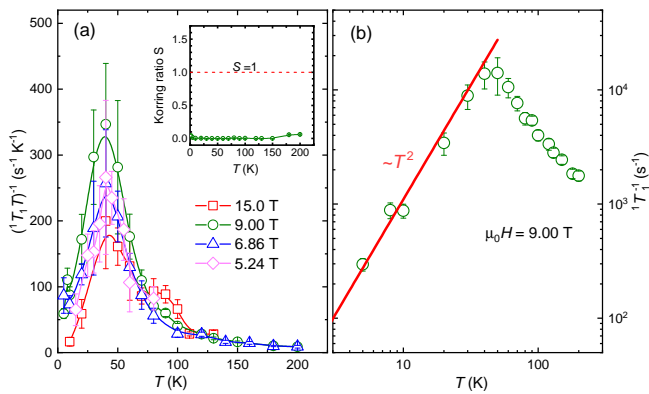


FIG. 3: (a) Measured $1/^{1}\text{T}_1T$ with temperature of $\text{Nd}_{0.85}\text{Sr}_{0.15}\text{NiO}_2$ under different fields. Inset: The Korringa ratio S (see text) as a function of temperature at 9 T. The guide line $S = 1$ roughly separates the regions of ferromagnetic fluctuations ($S > 1$) and AFM region ($S < 1$). (b) The low-temperature $1/^{1}\text{T}_1$ plotted in a log-log scale. The solid line is a function fit to $1/T_1 \sim T^{-2}$.

jection of local hyperfine fields along the external field is also randomly distributed between negative and positive values when the crystalline orientations are random in powders. Furthermore, since the FWHM still does not saturate down to 2 K, we think that the ordering is likely to be a quasi-static one where the ordered moments is not saturated yet. This is further discussed below.

The spin-lattice relaxation rate $1/T_1$, defined as, $1/T_1T = \lim_{\omega \rightarrow 0} \sum_q A_{\text{hf}}(q) \text{Im}\chi(q, \omega)/\omega$, where $\chi(q, \omega)$ is the dynamical susceptibility and $A_{\text{hf}}(q)$ the hyperfine coupling, is a sensitive probe of low-energy spin fluctuations [28]. Since ^1H nuclear spin is $1/2$, the spin-lattice relaxation rate $1/T_1$ of ^1H is only sensitive to magnetic fluctuations. The ^1H spin-lattice relaxation rate is then measured, and $1/T_1T$ as a function of temperature under various fields are plotted in Fig. 3. Upon warming from 2 K, the $1/^{1}\text{T}_1T$ first increases dramatically, then forms a peaked feature at $T \approx 40$ K, and finally flattens out at temperatures above 100 K.

To resolve the nature of the spin fluctuations, we calculated the Korringa ratio [29], $S = 4\pi k_B/\hbar(\gamma_n/\gamma_e)^2 K_s^2 T_1 T$, where γ_e and γ_n are the gyromagnetic ratio of electrons and nuclei, respectively. In principle, $S < 1$ ($S > 1$) indicates that the system contains dominant AFM (ferromagnetic) fluctuations. $S(T)$ curve under 9 T field is then shown in the inset of Fig. 3. The data fall in the regime far below the $S = 1$ line, which evidences dominant AFM fluctuations in the system over the entire measured temperature range.

A sharp peak in $1/^{1}\text{T}_1T$ is usually a signature of magnetic phase transition. The observed broad peak at about 40 K in bulk $\text{Nd}_{0.85}\text{Sr}_{0.15}\text{NiO}_2$ suggests the absence of long-range magnetic order, in agreement with previous results [24–26]. Nevertheless, it indicates the on-

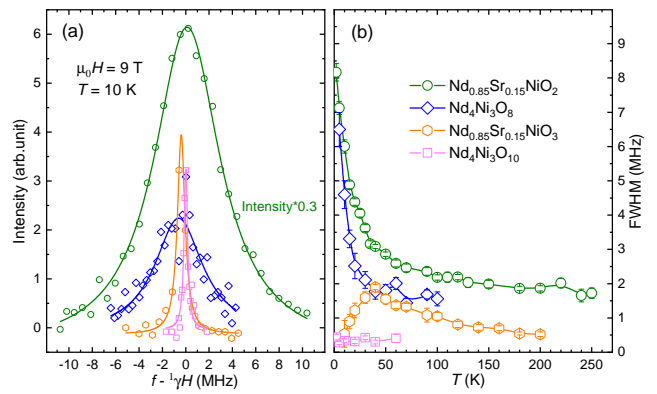


FIG. 4: (a) The ^1H spectra under a field of 9 T measured on four compounds of nickelates. The spectra are measured under identical condition, such as the same sample mass, coil, NMR pulse sequences, *etc.*. Solid lines are Lorentzian-form fit to the data. (b) Corresponding FWHM as functions of temperatures, obtained by the Lorentzian-form fit to the spectra.

set of low-energy spin fluctuations. Indeed, below 40 K, $1/^{1}\text{T}_1 \sim T^\alpha$, follows a power-law behavior, implying gapless spin excitations. As shown in Fig. 3(b), the power-law exponent $\alpha = 2$, close to the value of a system with AFM spin wave excitations ($\alpha = 5$ [30]). These results, together with the FWHM data, clearly evidence a developing quasi-static AFM order at low temperatures.

In order to understand the effects of hydrogen annealing and the origin of the ^1H signal, we performed comparative studies on four bulk nickelate compounds. $\text{Nd}_{0.85}\text{Sr}_{0.15}\text{NiO}_3$ [31] and $\text{Nd}_4\text{Ni}_3\text{O}_{10}$ [27] are made without hydrogen annealing, and $\text{Nd}_{0.85}\text{Sr}_{0.15}\text{NiO}_2$ and $\text{Nd}_4\text{Ni}_3\text{O}_8$ are synthesized after hydrogen annealing from the former two compounds [27, 32], respectively. Although NdNiO_3 is insulating and antiferromagnetically ordered below 200 K [33–36], $\text{Nd}_{0.85}\text{Sr}_{0.15}\text{NiO}_3$ shows a metallic behavior at low temperatures [31]. $\text{Nd}_4\text{Ni}_3\text{O}_{10}$ is also metallic at low temperatures [27, 37, 38], but $\text{Nd}_4\text{Ni}_3\text{O}_8$ [27] shows an insulating behavior at low temperatures and its magnetic properties remain unknown.

The spectra of the four compounds at a representative field 9 T are shown in Fig. 4(a). Interestingly, clear ^1H signals are resolved for the two samples without hydrogen annealing. This is not too surprising because hydrogen is hard to avoid in materials, given its small atomic size. However, the total integrated spectral weight of ^1H in $\text{Nd}_{0.85}\text{Sr}_{0.15}\text{NiO}_2$ is enhanced by a factor of ~ 45 compared with $\text{Nd}_{0.85}\text{Sr}_{0.15}\text{NiO}_3$, which suggests much higher hydrogen concentration in the annealed sample. However, by comparing to some organic materials, the concentration of hydrogen in $\text{Nd}_{0.85}\text{Sr}_{0.15}\text{NiO}_2$ is estimated to be less than 1%. Though largely enhanced after annealing, the level of hydrogen concentration remains small and can not provide an effective carrier doping. We also tried proton injection by using the ionic liquid method [39, 40], but no additional effect was ob-

served, implying a similar hydrogen concentration. On the other hand, the measured NMR spin-lattice relaxation rate takes a typical value about 1000 s^{-1} for temperatures between 10 K and 200 K, which is much larger than that of the environmental protons, indicating that the hydrogen ions strongly couple to the magnetic moment in the sample. Therefore, instead of providing effective doping, hydrogen entered in the system serves as a sensitive local probe for the magnetic properties of the system.

The respective FWHM of the ^1H NMR spectra of four compounds are shown in Fig. 4(b). For the annealed compounds, the FWHM are very large. For example, in $\text{Nd}_{0.85}\text{Sr}_{0.15}\text{NiO}_2$ the FWHM above 50 K corresponds to 0.5% of the resonance frequency, which is over twenty times of the hyperfine shift ($\sim 0.02\%$). The FWHM of $\text{Nd}_{0.85}\text{Sr}_{0.15}\text{NiO}_2$ and $\text{Nd}_4\text{Ni}_3\text{O}_8$ are much larger than those of unannealed samples. In particular, the FWHM in $\text{Nd}_4\text{Ni}_3\text{O}_8$ shows a large upturn below 40 K, similar to $\text{Nd}_{0.85}\text{Sr}_{0.15}\text{NiO}_2$. The larger FWHM reflects stronger inhomogeneity of the annealed compounds. The origin of the inhomogeneity is two-fold. On one hand, during annealing, the removal of apical oxygen may be incomplete, and the hydrogen and Ni ions may even form Ni-H bond [41]. These can certainly increase the level of inhomogeneity in the system. Inhomogeneity promotes the localization of electrons, which explains the observed insulating behavior up to room temperature in the annealed samples. On the other hand, the prominent upturn of FWHM below 40 K in the annealed samples should be associated with magnetic fluctuations, because at low temperatures the charge and structural inhomogeneities are quenched and can not account for such a strong temperature dependence.

In the following, we discuss the nature of the observed AFM fluctuations in bulk $\text{Nd}_{0.85}\text{Sr}_{0.15}\text{NiO}_2$. Although the magnetization data revealed a spurious ferromagnetic phase in both $\text{Nd}_{0.85}\text{Sr}_{0.15}\text{NiO}_2$ [23] and $\text{Nd}_4\text{Ni}_3\text{O}_8$ [27, 37], its high onset temperature (above 300 K) and the ferromagnetic nature are incompatible with our observation. As for the $4f$ electrons of Nd^{3+} , they are most likely disordered because of their weak hybridization with other electrons. These moments should be polarized under a finite magnetic field and hence can not contribute a large FWHM at low temperatures. With these considerations, and taking into account the insulating behavior of the annealed samples, we believe that the observed AFM fluctuations and quasi-static order are associated with the Ni local moments. The broad peak of $1/T_1T$ at around 40 K indicates the strength of magnetic couplings is at the order of 10 meV. Indeed, the superexchange coupling among nearest Ni moments is estimated theoretically to be 10-30 meV [5, 6, 14, 15], consistent with our observations.

Our results support the existence of antiferromagnetically interacting Ni moments and are consistent with the

doped Mott insulator scenario of nickelates. The onset of quasi-static ordering at 40 K coincides with the upturn of the low-temperature resistivity [23], which suggests an enhanced insulating behavior through magnetic scattering, as seen in quasi-1D Bechgaard salts [42]. A recent RIXS measurement suggests the doped hole results in a low-spin state of the Ni $3d^8$ configuration [43], which is also consistent with this picture. Nonetheless, the alternative picture, in which the doped hole leads to a high-spin $3d^8$ Ni configuration [22, 44], cannot be differentiated from our current data. Measurements on how the AFM fluctuations and quasi-static order evolve with different rare earth and/or hole doping would tell more information on whether a low-spin or a high-spin configuration is favored. As an interesting proposal, the Ni^{+1} moments could hybridize with Nd $5d$ itinerant electrons to form Kondo singlets [11]. In $\text{Nd}_{0.85}\text{Sr}_{0.15}\text{NiO}_2$, we do not observe an effect of Kondo-singlet formation which would cause a constant $1/T_1T$ at low temperatures [45]. A likely picture could be the Nd $5d$ bands are already emptied by the hole doping of Sr^{2+} at $x = 0.15$, and the Kondo effect would be more relevant in the underdoped regime. Interestingly, the FWHM with temperature of $\text{Nd}_{0.85}\text{Sr}_{0.15}\text{NiO}_3$ shows a peak at about 40 K and drops rapidly at low temperatures (Fig. 4(b)). Whether the Kondo physics is relevant there deserves further study.

Finally, we discuss the implication to superconductivity of the nickelate. The observation of AFM fluctuations and quasi-static magnetic ordering in the bulk materials suggests that the superconductivity in the nickelate is mediated via spin fluctuations, analogous to cuprates and iron-based superconductors. In the bulk materials, the absence of superconductivity and long-range antiferromagnetism would imply strong competition between several ordered phases, while the strong inhomogeneity in the system prevents formation of any long-range order. As for the films, similar AFM fluctuations are expected, from which superconductivity emerges. However, some factors could be unique to the films. First, with typical thickness of $\sim 10 \text{ nm}$ [1, 2], it should be easier to achieve oxygen homogeneity upon annealing, and a more homogeneous environment helps acquiring the phase coherence for superconductivity. Indeed, in superconducting $\text{Nd}_{0.8}\text{Sr}_{0.2}\text{NiO}_2$ films the resistivity remains metallic up to room temperature [2], indicating a much higher level of electron homogeneity. Furthermore, the SrTiO_3 substrate may provide additional doping or other interfacial effects to suppress the static AFM order and induce superconductivity in thin films. An example of the interface enhanced superconductivity has been realized in the single-layer FeSe film grown on the SrTiO_3 substrates [46, 47].

To summarize, we have performed ^1H NMR measurements on the hydrogen-annealed powdered $\text{Nd}_{0.85}\text{Sr}_{0.15}\text{NiO}_2$ samples, and observed enhanced AFM fluctuations below 100 K and emergence of a quasi-static

AFM order below 40 K. These properties are inherent to the strong correlations of Ni magnetic moments in $\text{Nd}_{0.85}\text{Sr}_{0.15}\text{NiO}_2$. Although superconductivity and long-range AFM order are not observed, likely due to the high inhomogeneity after annealing, the finding of strong AFM fluctuations pave the way for the understanding of superconductivity in nickelates.

This work is supported by the Ministry of Science and Technology of China with Grant Nos. 2016YFA0300504 and 2016YFA0300401, the National Natural Science Foundation of China with Grant Nos. 51872328, 11674392 and A0402/11927809, China Postdoctoral Science Foundation with Grant No. 2020M680797, the Fundamental Research Funds for the Central Universities, and the Research Funds of Renmin University of China with Grant Nos. 18XNLG24 and 20XNLG19.

* These authors contributed equally to this study.

† Electronic address: rong.yu@ruc.edu.cn

‡ Electronic address: hhwen@nju.edu.cn

§ Electronic address: wqyu-phy@ruc.edu.cn

- [1] D. Li, K. Lee, B. Wang, M. Osada, S. Crossley, H. R. Lee, Y. Cui, Y. Hikita, and H. Y. Hwang, *Superconductivity in an infinite-layer nickelate*, **Nature** **572**, 624 (2019).
- [2] D. Li, B. Wang, K. Lee, S. P. Harvey, M. Osada, B. H. Goodge, L. F. Kourkoutis, and H. Y. Hwang, *Superconducting Dome in $\text{Nd}_{1-x}\text{Sr}_x\text{NiO}_2$ Infinite Layer Films*, **Phys. Rev. Lett.** **125**, 027001 (2020).
- [3] M. Azuma, Z. Hiroi, M. Takano, Y. Bando, and Y. Takeda, *Superconductivity at 110 K in the infinite-layer compound $(\text{Sr}_{1-x}\text{Ca}_x)_{1-y}\text{CuO}_2$* , **Nature** **356**, 775 (1992).
- [4] V. I. Anisimov, D. Bukhvalov, and T. M. Rice, *Electronic structure of possible nickelate analogs to the cuprates*, **Phys. Rev. B** **59**, 7901 (1999).
- [5] A. S. Botana and M. R. Norman, *Similarities and Differences between LaNiO_2 and CaCuO_2 and Implications for Superconductivity*, **Phys. Rev. X** **10**, 011024 (2020).
- [6] A. Fujimori, *Electronic structure, magnetism, and superconductivity in infinite-layer nickelates*, **Journal Club for Condensed Matter Physics** **10**.36471 (2019).
- [7] Z.-J. Liang, R. Jiang, and W. Ku, *Where do the doped hole carriers reside in the new superconducting nickelates?* [arXiv:2005.00022](https://arxiv.org/abs/2005.00022) (2020).
- [8] Michael R. Norman, *Entering the Nickel Age of Superconductivity*, **Physics** **13**, 85 (2020).
- [9] S. Ryee, H. Yoon, T. J. Kim, M. Y. Jeong, and M. J. Han, *Induced magnetic two-dimensionality by hole doping in the superconducting infinite-layer nickelate $\text{Nd}_{1-x}\text{Sr}_x\text{NiO}_2$* , **Phys. Rev. B** **101**, 064513 (2020).
- [10] X. Wu, D. D. Sante, T. Schwemmer, W. Hanke, H. Y. Hwang, S. Raghu, and R. Thomale, *Robust $d_{x^2-y^2}$ -wave superconductivity of infinite-layer nickelates*, **Phys. Rev. B** **101**, 060504(R) (2020).
- [11] G.-M. Zhang, Y.-F. Yang, and F.-C. Zhang, *Self-doped Mott insulator for parent compounds of nickelate superconductors*, **Phys. Rev. B** **101**, 020501(R) (2020).
- [12] B. H. Goodge, D. Li, M. Osada, B. Y. Wang, K. Lee, G. A. Sawatzky, H. Y. Hwang, L. F. Kourkoutis, *Doping evolution of the Mott-Hubbard landscape in infinite-layer nickelates*, [arXiv:2005.02847](https://arxiv.org/abs/2005.02847) (2020).
- [13] J. Karp, A. Hampe, M. Zing, A. S. Botana, H. Park, M. R. Norman, and A. J. Millis, *A Comparative Many-Body Study of $\text{Pr}_4\text{Ni}_3\text{O}_8$ and NdNiO_2* , [arXiv:2010.02856](https://arxiv.org/abs/2010.02856).
- [14] M. Jiang, M. Berciu, and G. A. Sawatzky, *Critical Nature of the Ni Spin State in Doped NdNiO_2* , **Phys. Rev. Lett.** **124**, 207004 (2020).
- [15] A. E. Bocquet, T. Mizokawa, K. Morikawa, A. Fujimori, S. R. Barman, K. Maiti, D. D. Sarma, Y. Tokura, and M. Onoda, *Electronic structure of early 3d-transition-metal oxides by analysis of the 2p core-level photoemission spectra*, **Phys. Rev. B** **53**, 1161 (1996).
- [16] M. Hepting, D. Li, C. J. Jia, H. Lu, E. Paris, Y. Tseng, X. Feng, M. Osada, E. Been, Y. Hikita, Y.-D. Chuang, Z. Hussain, K. J. Zhou, A. Nag, M. Garcia-Fernandez, M. Rossi, H. Y. Huang, D. J. Huang, Z. X. Shen, T. Schmitt, H. Y. Hwang, B. Moritz, J. Zaanen, T. P. Devereaux, and W. S. Lee, *Electronic structure of the parent compound of superconducting infinite-layer nickelates*, **Nat. Mater.** **19**, 381 (2020).
- [17] K.-W. Lee and W. E. Pickett, *Infinite-layer LaNiO_2 : Ni^{1+} is not Cu^{2+}* , **Phys. Rev. B** **70**, 165109 (2004).
- [18] M.-Y. Choi, K.-W. Lee, and W. E. Pickett, *Role of 4f states in infinite-layer NdNiO_2* , **Phys. Rev. B** **101**, 020503(R) (2020).
- [19] Y. Gu, S. Zhu, X. Wang, J. Hu, and H. Chen, *A substantial hybridization between correlated Ni-d orbital and itinerant electrons in infinite-layer nickelates*, **Commun. Phys.** **3**, 84 (2020).
- [20] J. Chaloupka and G. Khaliullin, *Orbital Order and Possible Superconductivity in $\text{LaNiO}_3/\text{LaMO}_3$ Superlattices*, **Phys. Rev. Lett.** **100**, 016404 (2008).
- [21] P. Mandal, R. K. Patel, D. Rout, R. Banerjee, R. Bag, K. Karmakar, A. Narayan, J. W. Freeland, S. Singh, and S. Middey, *Giant orbital polarization of Ni^{2+} in square planar environment*, [arXiv:2009.02917](https://arxiv.org/abs/2009.02917).
- [22] Y. Wang, C.-J. Kang, H. Miao, and G. Kotliar, *Hund's metal physics: From SrNiO_2 to LaNiO_2* , **Phys. Rev. B** **102**, 161118(R) (2020).
- [23] Q. Li, C. He, J. Si, X. Zhu, Y. Zhang, and H.-H. Wen, *Absence of superconductivity in bulk $\text{Nd}_{1-x}\text{Sr}_x\text{NiO}_2$* , **Commun. Mater.** **1**, 16 (2020).
- [24] M. A. Hayward, M. A. Green, M. J. Rosseinsky, and J. Sloan, *Sodium Hydride as a Powerful Reducing Agent for Topotactic Oxide Deintercalation: Synthesis and Characterization of the Nickel(I) Oxide LaNiO_2* , **J. Am. Chem. Soc.** **121**, 8843 (1999).
- [25] M. A. Hayward and M. J. Rosseinsky, *Synthesis of the infinite layer Ni(I) phase NdNiO_{2+x} by low temperature reduction of NdNiO_3 with sodium hydride*, **Solid State Sci.** **5**, 839 (2003).
- [26] B.-X. Wang, H. Zheng, E. Krivyakina, O. Chmaissem, P. P. Lopes, J. W. Lynn, L. C. Gallington, Y. Ren, S. Rosenkranz, J. F. Mitchell, and D. Phelan, *Synthesis and characterization of bulk $\text{Nd}_{1-x}\text{Sr}_x\text{NiO}_2$ and $\text{Nd}_{1-x}\text{Sr}_x\text{NiO}_3$* , **Phys. Rev. Materials** **4**, 084409 (2020).
- [27] Q. Li, C. He, X. Zhu, J. Si, X. Fan, and H.-H. Wen, *Contrasting physical properties of the trilayer nickelates $\text{Nd}_4\text{Ni}_3\text{O}_{10}$ and $\text{Nd}_4\text{Ni}_3\text{O}_8$* , [arXiv:2006.10988](https://arxiv.org/abs/2006.10988).
- [28] T. Moriya, *The effect of electron-electron interaction on the nuclear spin relaxation in metals*, **J. Phys. Soc. Jpn.** **18**, 516 (1963).
- [29] Y. Nakai, K. Ishida, Y. Kamihara, M. Hirano, and

- H. Hosono, *Spin Dynamics in Iron-Based Layered Superconductor*($La_{0.87}Ca_{0.13}FePO$ Revealed by ^{31}P and ^{139}La NMR Studies, *Phys. Rev. Lett.* **101**, 077006 (2008).
- [30] A. Abragam, *Principles of Nuclear Magnetism* (Oxford University Press, Oxford, 1961).
- [31] J. A. Alonso, M. J. Martínez-Lope, and M. A. Hidalgo, *Hole and Electron Doping of $RNiO_3$ ($R=La, Nd$)*, *J. Solid State Chem.* **116**, 146 (1995).
- [32] R. Retoux, J. Rodriguez-Carvaja, and P. Lacorre, *Neutron Diffraction and TEM Studies of the Crystal Structure and Defects of $Nd_4Ni_3O_8$* , *J. Solid State Chem.* **140**, 307 (1998).
- [33] A. D. Caviglia, M. Först, R. Scherwitzl, V. Khanna, H. Bromberger, R. Mankowsky, R. Singla, Y.-D. Chuang, W. S. Lee, O. Krupin, W. F. Schlotter, J. J. Turner, G. L. Dakovski, M. P. Minitti, J. Robinson, V. Scagnoli, S. B. Wilkins, S. A. Cavill, M. Gibert, S. Gariglio, P. Zubko, J.-M. Triscone, J. P. Hill, S. S. Dhesi, and A. Cavalleri, *Photoinduced melting of magnetic order in the correlated electron insulator $NdNiO_3$* , *Phys. Rev. B* **88**, 220401(R) (2013).
- [34] D. Kumar, K. P. Rajeev, J. A. Alonso, and M. J. Martínez-Lope, *Spin-canted magnetism and decoupling of charge and spin ordering in $NdNiO_3$* , *Phys. Rev. B* **88**, 014410 (2013).
- [35] M. K. Hooda and C. S. Yadav, *Electronic properties and the nature of metal insulator transition in $NdNiO_3$ prepared at ambient oxygen pressure*, *Physica B* **491**, 31 (2016).
- [36] V. Scagnoli, U. Staub, Y. Bodenthin, M. García-Fernández, A. M. Mulders, G. I. Meijer, and G. Hammerl, *Induced noncollinear magnetic order of Nd^{3+} in $NdNiO_3$ observed by resonant soft x-ray diffraction*, *Phys. Rev. B* **77**, 115138 (2008).
- [37] B.-Z. Li, C. Wang, P. T. Yang, J. P. Sun, Y.-B. Liu, J. Wu, Z. Ren, J.-G. Cheng, G.-M. Zhang, and G.-H. Cao, *Metal-to-metal transition and heavy-electron state in $Nd_4Ni_3O_{10-\delta}$* , *Phys. Rev. B* **101**, 195142 (2020).
- [38] A. Olafsen, H. Fjellvåg, and B. C. Hauback, *Crystal Structure and Properties of $Nd_4Co_3O_{10+\delta}$ and $Nd_4Ni_3O_{10-\delta}$* , *J. Solid State Chem.* **151**, 46 (2000).
- [39] Y. Cui, G. Zhang, H. Li, H. Lin, X. Zhu, H.-H. Wen, G. Wang, J. Sun, M. Ma, Y. Li, D. Gong, T. Xie, Y. Gu, S. Li, H. Luo, P. Yu, and W. Yu, *Protonation induced high- T_c phases in iron-based superconductors evidenced by NMR and magnetization measurements*, *Sci. Bull.* **63**, 11 (2018).
- [40] Y. Cui, Z. Hu, J. Zhang, W. Ma, M. Ma, Z. Ma, C. Wang, J. Yan, J. Sun, J. Cheng, S. Jia, Y. Li, J. Wen, H. Lei, P. Yu, W. Ji, and W. Yu, *Ionic-Liquid gating induced protonation and superconductivity in $FeSe$, $FeSe_{0.93}S_{0.07}$, $ZrNCl$, $1T-TaS_2$ and Bi_2Se_3* , *Chin. Phys. Lett.* **36**, 077401 (2019).
- [41] L. Si, W. Xiao, J. Kaufmann, J. M. Tomczak, Y. Lu, Z. Zhong, and K. Held, *Topotactic Hydrogen in Nickelate Superconductors and Akin Infinite-Layer Oxides ABO_2* , *Phys. Rev. Lett.* **124**, 166402 (2020).
- [42] A. G. Lebed (Ed.), *The Physics of Organic Superconductors and Conductors*, (Springer Series in Materials Science, Vol. 110, Springer, 2008).
- [43] M. Rossi, H. Lu, A. Nag, D. Li, M. Osada, K. Lee, B. Y. Wang, S. Agrestini, M. Garcia-Fernandez, Y.-D. Chuang, Z. X. Shen, H. Y. Hwang, B. Moritz, K.-J. Zhou, T. P. Devereaux, and W. S. Lee, *Orbital and spin character of doped Carriers in infinite-layer nickelates*, [arXiv:2011.00595](https://arxiv.org/abs/2011.00595) (2020).
- [44] Y.-H. Zhang and A. Vishwanath, *Type-II t - J model in superconducting nickelate $Nd_{1-x}Sr_xNiO_2$* , *Phys. Rev. Research* **2**, 023112 (2020).
- [45] A. C. Hewson, *The Kondo Problem to Heavy Fermions*, (Cambridge University Press, 2009).
- [46] Q.-Y. Wang, Z. Li, W.-H. Zhang, Z.-C. Zhang, J.-S. Zhang, W. Li, H. Ding, Y.-B. Ou, P. Deng, K. Chang, J. Wen, C.-L. Song, K. He, J.-F. Jia, S.-H. Ji, Y.-Y. Wang, L.-L. Wang, X. Chen, X.-C. Ma, and Q.-K. Xue, *Interface-Induced High-Temperature Superconductivity in Single Unit-Cell $FeSe$ Films on $SrTiO_3$* , *Chin. Phys. Lett.* **29**, 037402 (2012).
- [47] Z.-X. Li, F. Wang, H. Yao, and D.-H. Lee, *What makes the T_c of monolayer $FeSe$ on $SrTiO_3$ so high: a sign-problem-free quantum Monte Carlo study*, *Sci. Bull.* **61**, 925 (2016).